Magazine of Civil Engineering

ISSN 2071-0305

journal homepage: http://engstroy.spbstu.ru/

DOI: 10.18720/MCE.95.5

Attenuation of the soil vibration amplitude at pile driving

A.O. Kolesnikov[a*], T.N. Kostiuk[a], V.N. Popov[b]

[a] *Novosibirsk State University of Architecture and Civil Engineering (Sibstrin), Novosibirsk, Russia*

[b] *Khristianovich Institute of Theoretical and Applied Mechanics SB RAS, Novosibirsk, Russia*

** E-mail: ao_kolesnikov@mail.ru*

Keywords: pile driving, attenuation of vibration, soil vibration, wave dispersion, portable vibration apparatus, structural damage, dynamic effect zone

Abstract. The paper presents the solution of the wave equation describing the attenuation of the vibration amplitude in the soil during pile driving. It is suggested that in the soil there is the area around the pile where the energy dissipates due to plastic deformations, and then the areas of the elastic state where surface waves propagate. In the framework of the wave model, the connections have been determined between vertical vibrations of the embedded solid body circular in plane and the motions in the area of the elastic soil state which is described by an integrity of infinitely thin layers. The interaction of the pile and soil in the plastic deformations area is beyond our consideration, though its size is of high importance for the problem solution. The formula has been derived, which permits, having the result of amplitude measurement in any point by a vibrometer and the position of surface wave propagation boundary, evaluating the soil vibrations at different distances from the pile driving point. The quantitative and qualitative agreement of the measured amplitudes and results of analysis obtained during test pile embedment performed during field measurements and found in references proves that the proposed model can be used to increase the accuracy of evaluation of the vertical soil vibrations.

1. Introduction

Equipment used in construction works is usually the source of vibrations propagating around. Regarding the type of the dynamic loading, the vibrations with high amplitudes and low frequencies may appear (for example, pile embedment in the soil), or the vibrations with relatively low amplitudes and high frequencies (for example, vibration embedment of pile curtains, vibrating rollers performance, etc.) Builders often do not have enough data on the choice of the equipment for pile or sheet pile embedment, nor on the parameters of the equipment performance needed to minimize the action of the propagating vibrations on buildings and people. Along with it, according to [1], the accuracy of vibration prediction by modern methods is insufficient. Errors in the choice of the equipment generating vibrations and the distance to the pile embedment site may cause not only worse conditions of existing buildings and constructions performance, but also the damages provoking the faster wear of these objects. Each worksite is unique, so one must take into account its specific conditions. Calculations and predictions, along with the dynamic monitoring of soils, buildings and constructions prevent troubles related with vibrations in building objects.

Thus, the modern standards [2–5] specify the requirements limiting the level of vibrations for neighboring buildings. In the case when the pile driving is performed close to them, there are restrictions of the velocity and acceleration of the foundation vertical vibrations with due regard to the soil type and construction peculiarities of the building and structure. However, according to [6], damages of buildings are related with the maximal shears which area not necessarily coincides with the area of the maximal values of the shear velocities. Today, any information about the minimal distances safe for the neighboring buildings foundations during the pile driving is missing. In spite of the fact that vibrations during the pile driving or sheet pile vibrating embedment are being studied for quite a long time [6–38], further investigations of the wave propagation in the soil from the source are still needed.

Bornitz [8] offers the Golitsin formula [7] for the evaluation of the varying vibration amplitudes of the surface waves *A* between two points within the distances r_0 and r from the embedded pile

Kolesnikov, A.O., Kostiuk, T.N., Popov, V.N. Attenuation of the soil vibration amplitude at pile driving. Magazine of Civil Engineering. 2020. 95(3). Pp. 49–56. DOI: 10.18720/MCE.95.5

$$A = A_0 \sqrt{\frac{r_0}{r}} e^{-\delta(r - r_0)}, \quad (1)$$

where A_0 is the amplitude, for example at r_0 = 0.5 m, δ is the vibration damping coefficient which varies within the range of 0.02–0.10 m^{-1} regarding the soil properties. Formula (1) was initially found for the evaluation of damping low-frequency Rayleigh waves with big lengths generated by earthquakes, for which the damping coefficient δ weakly depends on the properties of the upper soil layers. However, from 1930ties, the formula is used for the evaluation of the soil shear amplitudes during the vibrations propagating from the pile driving [8], and the long-term practical verification of this formula showed the satisfactory agreement with the full-scale research data [9].

Today, there is no common approach in the aspect of evaluation of the soil vibration parameters during the impact pile embedment. There are however certain problems in the Golitsin formula application for the soil vibration determination during building from various industrial sources, since the generated waves have higher frequencies and shorter length as compared to the surface waves from earthquakes; the first ones propagate in the upper soil layers near the earth surface [10]. The information resulting from the researches shows that the coefficient δ depends on the vibration source energy, frequency of the waves propagating in the soil, the distance from the vibration source, and soil formation thickness. Experimental data show that the values of δ may vary by more than one order and even change the sign in different points on the earth surface.

According to [11], the parameter δ can be evaluated by the formula

$$\delta = 2\pi f D / V, \quad (2)$$

where D is the soil damping (Hz·s)-1 (D<<1), f is the vibration frequency (Hz), V is the velocity of wave propagation (m/s), which depends either on the surface wave velocity V_R , or on the transversal wave velocity V_s .

It follows from (2) that δ reduces along with the decrease of the vibration frequency and increase of the wave propagation rate, i.e. the low-frequency wave damps less than the high-frequency one [12]. The dependence of δ on the material characteristics is evident. With the aid of measurements in [13] it is shown that soft soil decreases the vibration level faster than the hard soil. According to [14], the soil damping value depends on the vibration amplitude, soil type, humidity and temperature. For example, humid sand damps the vibrations weaker than dry sand, and frozen soil weakens the vibrations worse than thawed soil.

The authors of [6, 15–17, 33] consider the soil vibration during the impact pile embedment and detect two zones – the near one (nonlinear-plastic) and the far one (elastic). It is believed that the energy dissipates in the near zone due to the plastic flows in the soil. In the far zone, the vibrations mainly consist of the surface waves, and the soil works in the elastic state [18, 19]. In [20–23] it is shown that near the source causing the vertical vibrations, the vertically polarized shear waves dominate, but, as the distance from the source rises, the Rayleigh waves are generated faster. In the near zone, the amplitude attenuation is stronger, than in the far zone.

The near zone is not studied well enough. Neither wave propagation inside this zone, nor its boundaries are detected precisely. As a rule, the width of the near zone is evaluated to range from one to several meters from the pile embedded [6, 20, 24]. It was found in [17] by means of simulation that the calculation results agreed better with the experimental data when the distance from the far zone start was equal to the half of the Rayleigh wave length $r_f = 0.5L_R$, which coincides with the conclusions of [25]. The Rayleigh wave length is determined as

$$L_R = \frac{V_R}{f},$$

f is the pile vibration frequency (Hz), V_R is the Rayleigh wave velocity which can be found with the aid of [26]

$$V_R \approx V_s \frac{0.87 + 1.12\nu}{1 + \nu},$$

where V_s is the transversal wave velocity (m/s), ν is the Poisson ratio. The value V_s is calculated in accordance with [27]

$$V_s = \sqrt{\frac{\mu}{\rho}} = \sqrt{\frac{E}{2\rho(1+\nu)}}.$$

Here, μ is the Lame coefficient equivalent to the shear module G, (Pa), ρ is the soil density (kg/m^3), E is the elasticity module (Pa).

When detecting the distance from the far zone start, the following approach is also applicable [28]. As the pile is being embedded in soil, the boundary r_f position changes. Each section of the pile lying at the depth h, is and source of longitudinal and transversal waves which impact over the earth surface and transform a part of energy into the Rayleigh waves. The distance from the pile to the point on the soil r_h, where the Rayleigh waves come from the source at the depth h is found by the expression

$$r_h = h\frac{V_R}{\sqrt{V_p^2 - V_R^2}},$$

where V_p is the longitudinal wave velocity calculated according to

$$V_p = \sqrt{\frac{\lambda + 2\mu}{\rho}}, \lambda = \frac{\nu E}{(1+\nu)(1-2\nu)}.$$

In this case, the position of the elastic zone boundary can be evaluated as $r_f < r_H$,

$$r_H = H\frac{V_R}{\sqrt{V_p^2 - V_R^2}},$$

where H is the depth of pile embedment in the soil.

Thus, since the evaluation of the dynamic actions is an important and urgent engineering task not only for the pile foundations construction but also for the design of the foundations for machines with dynamic loadings, the more accurate solutions of this task remains topical [29–31, 38]. In practice, it is desirable to have reliable results using quite simple relations in calculations. In this context, the present paper offers the formula to determine the law of vibrations attenuation as the distance from the source rises. The calculation results obtained by the formula are compared both with the experimental findings presented in [6, 24] and with the authors' results.

2. Methods

2.1. Theoretical method

We assume that, according to [6], the maximal soil shears are caused mainly by the waves propagating from the side pile surface. To determine the vibration attenuation law in the far zone, the wave model is used; in the framework of this model, we detect the links between the motions at the vertical vibrations of the embedded circular in plane absolute solid body and the motions in the surrounding soil. The contact with the medium is realized through the side surface of the embedded body. The medium described by the integrity of infinitely thin layers is considered as the soil. Hence, we solve the task of the vertical vibrations of the infinite plate with a circular cut.

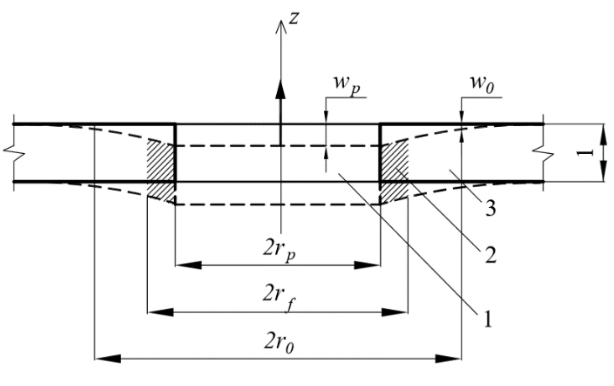

Figure 1. Schematic of the circular cut position in the vibrating thin plate:
1 – cut, 2 – nonlinear-plastic (near) zone, 3 – elastic (far) zone.

Let us consider the warping axisymmetric vibrations of the infinitely thin layer with one circular cut, it radius r_p (Fig. 1). In this case, the equation of elastic medium motion without volume forces in the cylindrical system of coordinates (r,θ,t) is written as:

$$\mu(\frac{1}{r}\frac{\partial}{\partial r}r\frac{\partial w}{\partial r}+\frac{1}{r^2}\frac{\partial^2 w}{\partial\theta^2})=\rho\frac{\partial^2 w}{\partial t^2}. \quad (3)$$

Here, $w=w(r,\theta,t)$ is the motion along the axis z, ρ is density. Proceeding from the medium motion character, presuming that every point remains on its straight line during the vibration $(r,\theta=const)$, and the distance between them does not change, the equation (3) can be transformed as

$$\frac{1}{r}\frac{\partial}{\partial r}r\frac{\partial w}{\partial r}=\frac{\rho}{\mu}\frac{\partial^2 w}{\partial t^2}, \quad (4)$$

under the condition of the space $r_0\geq r_p$ in a certain point

$$w(r_0,t)=w_0e^{i\omega t}. \quad (5)$$

Since we consider the vibrations of the absolute solid body, every point of which in plane $(0\leq r\leq r_p)$ shear by the same value, let us pass to the coordinate $r=r-r_p$. In this case, the equation (4) remains as it is written. This would be enough when considering the embedded solid body under the dynamic loadings, assuming the properties of the elastic medium in the near and far zones. If we presume the presence of the near (nonlinear-plastic) zone with the external boundary $r=r_f$, it is advisable (4) to consider in the area $r\geq r_f$ at $r_0\geq r_f$ and to pass to the new coordinate like $r=r-r_f$.

The solution of (4), (5) is carried out by the variable separation method and, according to [39], can be presented as

$$w=e^{i\omega t}\sum_{n=0}^{\infty}[A_nH_n^{(1)}(kr)+B_nH_n^{(2)}(kr)]. \quad (6)$$

where $k=\omega/\sqrt{\mu/\rho}$, $H_n^{(1)}$, $H_n^{(2)}$ are the first and second kind Hankel functions , and A_n, B_n are the constant coefficients to be determined.

Since we consider the plane with one cut, and there are no other source of vibration, then (6) describes only divergent waves at $r\to\infty$. It follows from the asymptotic expansions of the Hankel functions [39] that this conditions at the time factor $e^{i\omega t}$ is satisfied by the function $H_n^{(2)}$ and hence, $A_n=0$. It follows from the axial symmetry condition that $n=0$. Then we have $w=e^{i\omega t}B_0H_0^{(2)}(kr)$, where, according to (5)

$$B_0=w_0\big/H_0^{(2)}(kr_0),$$

and hence,

$$w=e^{i\omega t}\,w_0H_0^{(2)}(kr)\big/H_0^{(2)}(kr_0).$$

Let us evaluate the relative motion of the soil w/w_0 using the relation

$$w/w_0=H_0^{(2)}(kr)/H_0^{(2)}(kr_0)=S_R(kr)+iS_I(kr),$$

where

$$S_R(kr)=\frac{J_0(kr)J_0(kr_0)+Y_0(kr)Y_0(kr_0)}{J_0^2(kr_0)+Y_0^2(kr_0)},\ \ S_I(kr)=\frac{J_0(kr)Y_0(kr_0)-Y_0(kr)J_0(kr_0)}{J_0^2(kr_0)+Y_0^2(kr_0)}.$$

In the initial system of coordinates, $S_R(kr)$ and $S_I(kr)$ look like

$$S_R(kr) = \frac{J_0\left[k\left(r-r_f\right)\right]J_0\left[k\left(r_0-r_f\right)\right]+Y_0\left[k\left(r-r_f\right)\right]Y_0\left[k\left(r_0-r_f\right)\right]}{J_0^2\left[k\left(r_0-r_f\right)\right]+Y_0^2\left[k\left(r_0-r_f\right)\right]},$$

$$S_I(kr) = \frac{J_0\left[k\left(r-r_f\right)\right]Y_0\left[k\left(r_0-r_f\right)\right]-Y_0\left[k\left(r-r_f\right)\right]J_0\left[k\left(r_0-r_f\right)\right]}{J_0^2\left[k\left(r_0-r_f\right)\right]+Y_0^2\left[k\left(r_0-r_f\right)\right]}.$$

Thus, the varying vibration amplitudes can be described by the formula

$$A = A_0(S_R^2 + S_I^2)^{0.5}, \tag{7}$$

where A_0 is the amplitude in the point r_0. Fig. 2 shows the results obtained in accordance with (7) at different dimensionless frequencies $a_0 = kr_0$ in the case $r_f = r_p,\ r_0 = r_p$. The calculation data illustrate the dynamics of amplitude variation in the medium, and particularly show that the low-frequency wave damps weaker than the waves with higher frequencies, which agrees with [12].

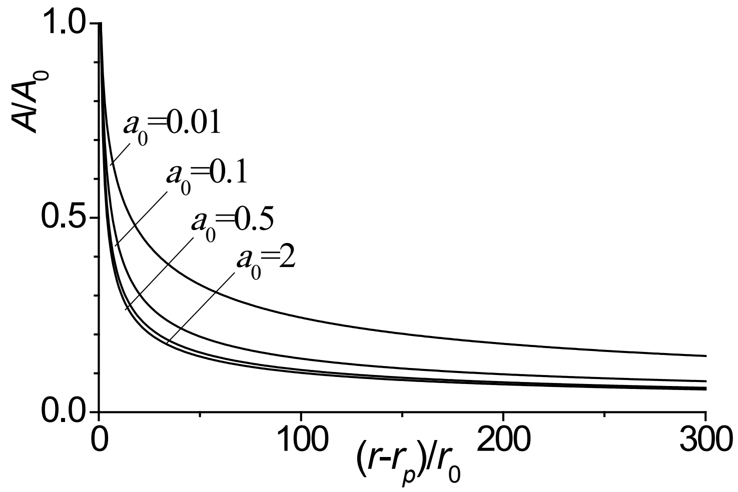

Figure 2. Attenuation of vibration amplitudes at various dimensionless frequencies a_0.

2.2. Experimental method

Experiments were carried out to analyze the dynamic actions occurring during the pile driving. Three similar-procedure series of tests were carried out. In each case, one prismatic assembled reinforced-concrete pile CP-1, CP-2, CP-3, the length 7.0 m, the cross section 30×30 cm, was embedded by the hydraulic hammer ROPAT. The vibration amplitudes and frequencies were registered on the soil surface in four points simultaneously with the embedment. The distances from the embedded pile center to the probe 1 was 1.5 m, to the probes 2, 3, 4 it was 10 m, 20 m, and 30 m, respectively. Every test pile was embedded directly in the soil from the ditch bottom.

The soil in the worksite from the ditch bottom surface down to the depth of 3.6 m consisted of non-subsiding solid sand clay with the average water saturation degree and density $\rho = 1.78$ t/m3, the deformation module $E_0 = 8.5$ MPa and Poisson ratio $\nu = 0.33$, subsoiled with fine uniform sand with the density $\rho =$ 2.01 t/m3, the deformation module $E_0 = 17.6$ MPa. The subterranean water at the test moment was at the depth of 3.5 m from the ditch bottom surface.

To register the vibration amplitudes and frequencies we used the vibration-measuring apparatus AVM-1, which includes 3D probes with vibrating accelerometers ADXL, AD/DA converter and PC. AVM-1 permits registering the vibrations and simultaneously process the gathered information. The probe presents a metal case shaped as a cube which can be fastened on the soil surface, with boards with integral two-channel accelerometers inside. The probes were connected to the AD/DA converter via cables. The external module E14-140 made by L-CARD was used as the AD/DA converter. The major engineering characteristics of the used apparatus are presented in the Table below. The data were registered for each embedded pile.

Table 1. Engineering characteristics of apparatus.

Frequency measurement range, Hz	1 – 100
Amplitude measurement range, mm	0.0005–20
The limit of allowed main relative error in the amplitude measurement, %	± 3
The limit of allowed main relative error in the frequency measurement in the range of 1–100 Hz	± 0.2 Hz
Amount of axis in the vibrating probe	3
Probe amount, pcs.	4
Process temperature range	From –10°C to +80°C

3. Results and Discussion

Fig. 3 shows the measurement and calculation results obtained by the formula (7): the rated vibration amplitudes $A / A_{\max}$ for various distances from the source $r = 1.5$; 10; 20; 30 m. The point within 10 m from the vibration source is used as r_0, for $A_{\max}$ we used the amplitude values at $r = 1.5$ m. The start of the elastic medium zone $r_f = 1$ m was chosen in the same way as in [24], where the soil vibration was studied during the embedment of the similar size pile. The solid lines in Fig. 3–5 show the calculation results obtained with the aid of (7), the dotted lines present the results obtained with the formula (1).

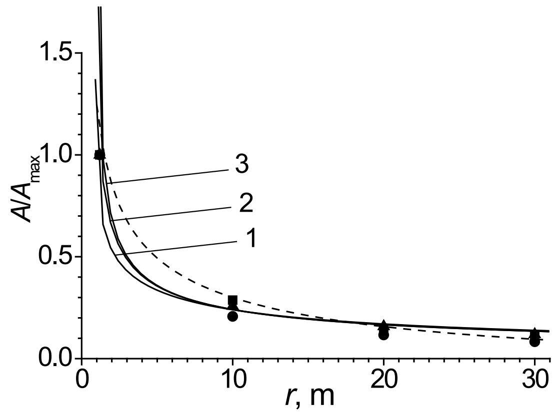

Figure 3. Attenuation of the relative vibration amplitude of the soil at various k = 0.1 (1), 0.5 (2), 2 (3) ■, ▲, ● – measurement data.

Fig. 3 demonstrates the satisfactory agreement between the calculations and measured data. It follows from the results of the full-scale and numerical experiments that, as the distance from the vibration source increases, the vibration amplitudes decrease monotonically. The fastest decreases of the amplitude takes place in the area close to the vibration source. For example, in respect to the nearest measurement point ($r = 1.5$ m) within 5 m from the vibration source, the amplitude decreases approximately by three times, by 4 times within 10 m, by 7 times within 20 m and by 10 times within 30 m. The strongest effect of the parameter k on the amplitude variation is observed at $r \leq 8$ м. At low k (for example, at the constant frequency and low density of the medium), the vibrations damp faster. As k rises, the damping is slower, and at $k \geq 0.5$, the obtained solutions feasibly coincide. In the area at $r > 8$, the attenuation does not depend on k. The curves in the figure going above $A/A_{\max} = 1$ describe the variations of the vibration amplitudes in the area between $r = 1.5$ m and $r = r_f$. The results obtained by the formula (1) at $\delta = 0.03$ m^{-1} [6] agree satisfactory with the data obtained during the measurements at $r \geq 10$ m. In the area of 3 m $\leq r \leq 9$ m, the discrepancy between the results given by the formulas (1) and (7) ranges from 20 to 30 %. However, no experimental data makes impossible to confirm the advantages of any method.

To evaluate the applicability of (7), the results of soil vibration amplitudes presented in [6, 24] were used. Fig. 4 demonstrates the measurement results [24] within different distances from the source $r = 1.5$; 5; 10; 15; 20; 25; 30 m and calculations of the rated vibration amplitudes $A / A_{\max}$. Similarly to the above version, $r_0 = 10$ m. The amplitude values at $r = 1.5$ m were used as $A_{\max}$. The start of the elastic medium zone $r_f = 1$ m as determined in [24] in accordance with the results of research of the soil vibrations during the pile driving. The calculations by the formula (1) were performed at $\delta = 0.04$ m^{-1} [6].

Figure 5 illustrates the measurement results from [6] at the distances from the source $r = 3$, 5, 10, 20, 30 m and calculations, according to (7), of the rated vibration amplitudes $A / A_{\max}$. The amplitude values at $r = 3$ m were used as $A_{\max}$. Again, $r_0 = 10$ m. The start of the elastic medium zone $r_f = 2$ m was chosen in [6] in accordance with the results of research of the soil vibrations during the pile driving. According to [6], the calculations with the formula (1) were carried out at $\delta = 0.07$ m^{-1}.

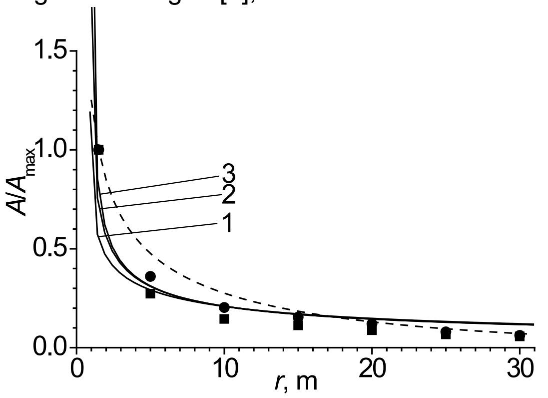

Figure 4. Attenuation of the relative vibration amplitude of the soil at $k =$ 0.1 (1), 0.5 (2), 2 (3) ■, ● – measurement data [24].

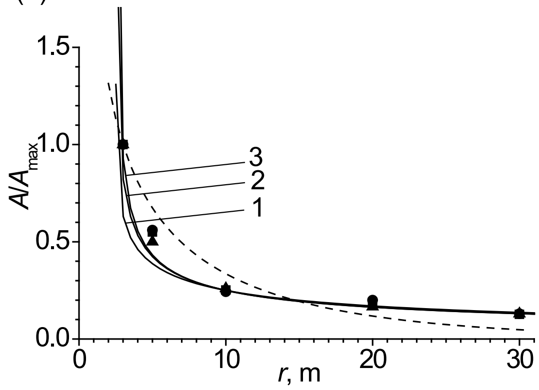

Figure 5. Attenuation of the relative vibration amplitude of the soil at $k =$ 0.1 (1), 0.5 (2), 2 (3) ■, ▲, ● – measurement data [6].

According to the results presented in Fig. 4, 5, there is the satisfactory agreement between the data calculated by the formula (7) and the data from [6, 24] to describe the variations in the vertical soil vibration amplitude versus the distance from the vibration source. The Golitsin's formula (1) gives a discrepancy between the exprerimental and calculation data; to reduce this discrepancy, one need information to correct the vibration attenuation coefficient δ which varies versus the distance from the source. Extra analysis of the soil vibration is needed. Thus, the wave model solution has an advantage over the formula (1).

4. Conclusions

The following conclusons are derived from the performed investigation:

1. The solution (7) of the wave model describes the variation in the soil vertical vibration amplitude versus the distance from the vibration source. To use this solution, it is enough to have the data of only one measurement of the vibration amplitude and the size of the non-linear-plastic area around the driven pile. The vibration amplitude should be measured within the distance exceeding the width of the non-linear-plastic zone, or on its boundary. The size of the non-linear-plastic area around the pile is evaluated approximaterly either by the half of the Rayleigh wave, or as a distance from 1 to 3 m.

2. Application of the formula (7) gives the satisfactory agreement of the calculation and measurement data in the field measurement and solutions of elastic-plastic problems involving big soft packages.

5. Acknowledgements

The research has been carried out within the Program of Fundamental Research of the State Academies of Sciences 2013-2020 (project No. AAAA-A17-117030610136-3).

References

1. Holscher, P., Waarts, P.H. Reliability of vibration prediction and reducing measures [Online]. Report Delft Cluster. Delft. 2003. URL: http://resolver.tudelft.nl/uuid:05863abb-5090-4399-a48b-ee04d26cd883
2. ISO 4866:2010. Mechanical vibration and shock – Vibration of fixed structures – Guidelines for the measurement of vibrations and evaluation of their effects on structures.
3. DIN 4150-3:2016-12. Vibrations in buildings – Part 3: Effects on structures.
4. BS 7385-2:1993. Evaluation and measurement for vibration in buildings – Part 2: Guide to damage levels from groundborne vibration.
5. NS 8141-1:2012+A1:2013 Vibration and shock – Guideline limit values for construction work, open-pit mining and traffic – Part 1: Effect of vibration and air blast from blasting on constructions, including tunnels and rock caverns.
6. Kalyuzhnyuk, M.M., Rud', V.K. Svaebojnye raboty pri rekonstrukcii [Piling works during reconstruction] [Online]. Saint-Petersburg: Strojizdat, 1989. 160 p. URL: http://science.totalarch.com/book/4482.rar (rus)
7. Golitsin, B.B. On dispersion and attenuation of seismic surface waves. Russian Academy of Science News. 1912. 6(2).
8. Bornitz, G. Über die ausbreitung der von großkolbenmaschinen erzeugten bodenschwingungen in die tiefe [Online]. Berlin. Springer-Verlag, 1931. 56 p. URL: https://DOI.org/10.1007/978-3-642-99597-2
9. Vasil'evskij, YU.I. Dinamika pogruzheniya zhelezobetonnyh svaj pri zabivke [Dynamics of reinforced concrete piles immersion during driving]. Trudy koordinacionnyh soveshchanij po gidrotekhnike. 1971. No. 66. Pp. 47–51. (rus)
10. Svinkin, M.R. Soil and structure vibrations from construction and industrial sources [Online]. Proceedings of the Sixth International Conference on Case Histories in Geotechnical Engineering. Omni Press, Arlington, Virginia. 2008. Pp. 1–14. URL: https://scholarsmine.mst.edu/icchge/6icchge/session13/8

11. Athanasopoulos, G.A., Pelekis, P.C., Anagnostopoulos, G.A. Effect of soil stiffness in the attenuation of Rayleigh-wave motions from field measurements. Soil Dynamics and Earthquake Engineering. 2000. 19(4). Pp. 277–288. DOI: 10.1016/S0267-7261(00)00009-9
12. Auersch, L., Said, S. Attenuation of ground vibrations due to different technical sources. Earthquake Engineering and Engineering Vibration. 2010. 9(3). Pp. 337–344. DOI: 10.1007/s11803-010-0018-0
13. Clough, G.W., Chameau, J-L. Measured effects of vibratory sheet pile driving [Online]. Journal of Geotechnical Engineering. Division, ASCE. 1980. 106(GT10). Pp. 1081–1099. URL: https:// search-works.stanford.edu/view/486385
14. Amick, H., Gendreau, M. Construction vibrations and their impact on vibration-sensitive facilities. Proceedings of the 6th ASCE Construction Congress. 2000. DOI: 10.1061/40475(278)80
15. Barkan, D.D. Dynamics of bases and foundations [Online]. New York: McGraw-Hill Book Company Inc., USA, 1962. 478 p. URL: https://archive.org/details/dynamicsofbasesf00bark
16. Massarsch, K.R. Effects of vibratory compaction [Online]. TransVib 2002 – International Conference on Vibratory Pile Driving and Deep Soil Compaction. 2002. Pp. 33–42. URL: https://www.researchgate.net/publication/292792536_Effects_of_vibratory_compaction
17. Darius, M., Stefan, V.B. A simple engineering soil surface vibration prediction method. Civil Engineering Research Journal. 2018. 4(2). DOI: 10.19080/CERJ.2018.04.555632
18. Massarsch, K.R. Vibrations caused by pile driving [Online]. The Magazine of the Deep Foundations Institute. Part 1: Summer Edition. 2004. Pp. 1–8. URL: https://ru.scribd.com/document/355361734/Vibrations-Caused-by-Pile-Driving
19. Whenham, V. Power transfer and vibrator-pile-soil interactions within the framework of vibratory pile driving. Doctoral Thesis [Online]. University of Louvain. Belgium. 2011. URL: http://hdl.handle.net/2078.1/75975
20. Head, J.M., Jardine, F.M. Ground-borne vibrations arising from piling [Online]. CIRIA Technical Note 142. Construction Industry Research and Information Association (CIRIA). London. 1992. URL: https://www.thenbs.com/PublicationIndex/documents/details?Pub=CIRIA&DocID=53095
21. Svinkin, M.R. Overcoming soil uncertainty in prediction of construction and industrial vibrations [Online]. Uncertainty in the geologic environment: from theory to practice. ASCE, Geotechnical Special Edition. 1996. No. 58. Pp. 1178–1194. URL: https://www.researchgate.net/publication/287095145_Overcoming_soil_uncertainty_in_prediction_of_construction_and_industrial_vibrations
22. Svinkin, M.R. Minimizing construction vibration effects. Practice Periodical on Structural Design and Construction, ASCE. 2004. 9(2). Pp. 108–115. DOI: 10.1061/(ASCE)1084-0680(2004)9:2(108)
23. Masoumi, H.R., Degrande, G. Numerical modeling of free field vibrations due to pile driving using a dynamic soil-structure interaction formulation. Journal of Computational and Applied Mathematics. 2008. 215(2). Pp. 503–511. DOI: 10.1016/j.cam.2006.03.051
24. Vasenin, V.A. Ocenka parametrov kolebanij grunta pri udarnom pogruzhenii svaj. Osnovnye sledstviya [Estimation of ground vibrations parameters during impact pile driving. The main investigation] [Online]. Rekonstrukciya gorodov i geotekhnicheskoe stroitel'stvo. 2003. No 7. Pp. 210–223. URL: https://cyberleninka.ru/article/n/eksperimentalnye-issledovaniya-parametrov-kolebaniy-grunta-pri-zabivke-svay (rus)
25. Wolf, J.P. Foundation vibration analysis using simple physical models. Prentice Hall, Upper Saddle River, USA, 1994. 464 p.
26. Holmberg, R., Arnberg, P.W., Bennerhult, O., et al. Vibrations generated by traffic and building construction activities. Swedish Council for Building Research. Stockholm, Sweden. 1984.
27. Massarsch, K.R. Settlements and damage caused by construction-induced vibrations [Online]. Proceedings of the International Workshop Wave 2000. Bochum, Germany. 2000. Pp. 299–315. URL: https://ru.scribd.com/document/37007330/Settlements-and-Damage-Caused-by-Construction-Induced-Vibrat
28. Dowding, C.H. Construction Vibrations. Prentice Hall. Upper Saddle River, USA, 1996. 620 p.
29. Cleary, J.C., Steward, E.J. Analysis of ground vibrations induced by pile driving and a comparison of vibration prediction methods. DFI Journal – The Journal of the Deep Foundations Institute. 2016. 10(3). Pp. 125–134. DOI: 10.1080/19375247.2017.1288855
30. Rahman, N., Musir, A.A., Dahalan, N., Ghani, A., Khalil, M. Review of vibration effect during piling installation to adjacent structure. AIP Conference Proceedings. 2017. No. 1901. 110009. DOI: 10.1063/1.5010550
31. Deckner, F., Viking, K., Hintze, S. Wave Patterns in the Ground: Case Studies Related to Vibratory Sheet Pile Driving. Geotechnical and Geological Engineering. 2017. 35(6). Pp. 2863–2878. DOI 10.1007/s10706-017-0285-x
32. Massarsch, K.R., Fellenius, B.N., Bodare, A. Fundamentals of the vibratory driving of piles and sheet piles. Geotechnik 40. 2017. No. 2. Pp. 126–141. DOI: 10.1002/gete.201600018
33. Khoubani, A., Ahmadi, M.M. Numerical study of ground vibration due to impact pile driving. Geotechnical Engineering. 2014. 167(1). Pp. 28–39. DOI: 10.1680/geng.11.00094
34. Jayawardana, P., Achuhan, R., Subashi De Silva, G.H.M.J., Thambiratnam, D.P. Use of in-filled trenches to screen ground vibration due to impact pile driving: experimental and numerical study. Heliyon. 2018. 4(8). DOI: 10.1016/j.heliyon.2018.e00726
35. Dungca, J.R., Acosta, D.Y., Juego, M.B., Sanchez, H.M., Sanchez, I.S. The propagation behavior of pile-driving-induced vibration done on soil at varying distances and its effects on existing structures. International Journal of GEOMATE. 2016. 10(21). Pp. 1877–1883. DOI: 10.21660/2016.21.5223
36. Li, Q., Shu, W., Cao, L., Duan, W., Zhou, B. Vertical vibration of a single pile embedded in a frozen saturated soil layer. Soil Dynamics and Earthquake Engineering. 2019. No. 122. Pp. 185–195. DOI: 10.1016/j.soildyn.2019.03.032
37. Dai, D., El Naggar, M.H., Zhang, N., Gao, Yu., Li, Zh. Vertical vibration of a pile embedded in radially disturbed viscoelastic soil considering the three-dimensional nature of soil. Computers and Geotechnics. 2019. No. 111. Pp. 172–180. DOI: 10.1016/j.compgeo.2019.03.013
38. Ter-Martirosyan, Z.G., Ter-Martirosyan, A.Z., Sobolev, E.S. Interaction of the pile and surrounding soil during vibration driving. IOP Conf. Series: Materials Science and Engineering. 2018. No. 456. DOI: 10.1088/1757-899X/456/1/012093
39. Tihonov, A.N., Samarskij, A.A. Uravneniya matematicheskoj fiziki [Equations of mathematical physics]. Moscow: Nauka, 1966. 724 p. (rus)

Contacts:

Aleksei Kolesnikov, ao_kolesnikov@mail.ru

Tatiana Kostiuk, tanyakostuk26@gmail.com

Vladimir Popov, popov@itam.nsc.ru